



Fermi National Accelerator Laboratory

FERMILAB-Conf-76/90-EXP
7100.180

SEARCH FOR NEW PARTICLES PRODUCED IN $\bar{\nu}_{\mu}$ NUCLEON INTERACTIONS IN THE 15-FOOT BUBBLE CHAMBER*

F. A. Nezrick

November 1976

Invited talk at the SLAC Summer Institute on Particle Physics,
October 2-13, 1976

*This experiment was performed by the following group: J. P. Berge, F. A. DiBianca, H. Emans, R. Hanft, C. Kochowski, F. A. Nezrick, W. G. Scott, W. Smart, and W. Venus, Fermilab; V. V. Ammosov, A. G. Denisov, P. F. Ermolov, V. A. Pitukhin, Y. G. Rjabov, E. A. Slobodyuk, and V. I. Sirotenko, IHEP, Serpukhov; V. I. Efremenko, P. A. Gorichev, V. S. Kaftanov, V. D. Khovansky, G. K. Kliger, V. Z. Kolganov, S. P. Krutchinin, M. A. Kubantsev, S. V. Mironov, A. N. Rosanov, and V. G. Shevchenko, ITEP, Moscow; C. T. Coffin, R. N. Diamond, H. French, W. Louis, B. P. Roe, A. A. Seidl, and D. Sinclair, University of Michigan.



INTRODUCTION

Preliminary results are presented on searches for new particles produced in the interaction of antineutrinos with nucleons in the 15-ft bubble chamber. Indirect tests for new particle production are made by investigating the x and y distributions of all charged current events and by investigating the general properties of events with neutral strange particles. Direct tests of new particle production are made by searching for dilepton events and by looking for peaks in the invariant mass distributions of events involving neutral strange particles.

EXPERIMENTAL CONFIGURATION

This experiment utilized the 15-ft bubble chamber filled with a 21% atomic neon-hydrogen mixture ($X_0 = 110$ cm) exposed to the horn focused antineutrino beam. The incident proton energy was 300 GeV and the average intensity was 8.5×10^{12} protons per pulse. The proton spill time was 20 μ seconds which optimally matched the good focusing time of the horn system. The horn system focused negative particles ($\pi^- \rightarrow \mu^- \bar{\nu}$) and defocused positive particles ($\pi^+ \rightarrow \mu^+ \nu$). To suppress even more the neutrino background in the antineutrino beam an "absorptive plug" was placed downstream of the first horn to remove the wrong sign mesons which passed through the hole in the horn. Figure 1 shows the relative importance of the "absorptive plug" in reducing the neutrino background. In this experiment the neutrino contamination was less than 4% of the total flux.

The external muon identifier (EMI) was used in this experiment. The EMI consists of approximately 600 gms cm^{-2} of zinc absorber and magnet coils inside the vacuum vessel of the bubble chamber followed by 23 m^2 of multiwire proportional chambers.¹ Muon candidates seen in the bubble chamber are extrapolated to the EMI in an attempt to match

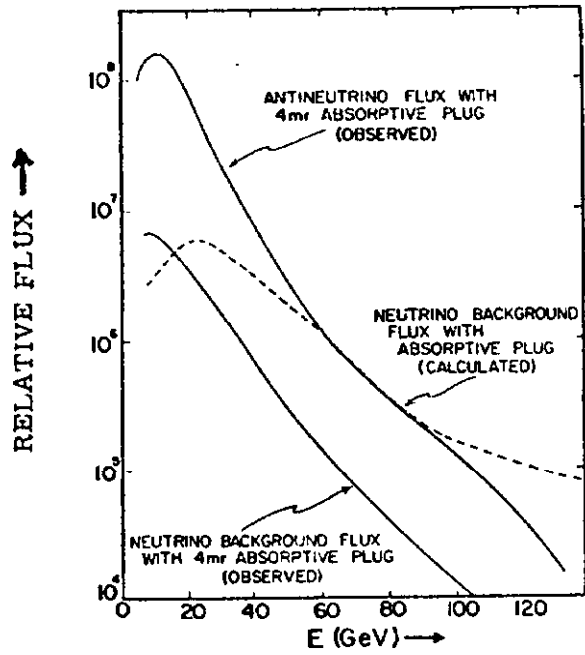


Fig. 1: Relative neutrino background flux with and without use of 4 mr absorptive plug compared with the antineutrino flux.

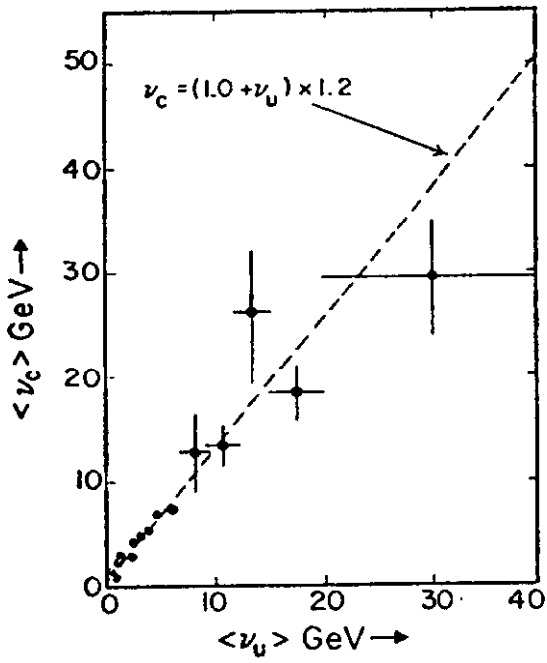


Fig. 2: Correction for missing hadronic energy.

Because of the geographical scale of this collaboration and our desire for a speedy result the bubble chamber film distribution received special attention. The entire quantity of film was copied using the direct reversal technique.³ There are no identified differences in measurements from the original or copied film. Each nation received 50% original film and 50% copied film but was responsible for scanning and measuring only the original film. The copied film was used for cross checking.

DATA ANALYSIS

Event Scan Selection: The film was scanned for all neutral induced events with a total momentum, (charged plus neutral), ΣP_x , along the neutrino beam direction greater than ~ 1 GeV. Events consisting of a single charged track only were not included in the scan. Therefore the elastic events $\bar{\nu} + p \rightarrow \mu^+ + n$ were not detected but those with observed ν^0 were recorded. About 3000 neutral candidates were found in the scan. Each of the four groups was responsible for scanning and measuring 25% of the total data. The Hydra Geometry program⁴ was used for geometrical reconstruction.

Muon Selection: The EMI is used to identify the muon tracks. After the event is measured in the bubble chamber all tracks which could be muons are extrapolated to the EMI. From the extrapolated position in the EMI, the multiple scattering circle (the tracks penetrate about ~ 600 g/cm² of absorber between the fiducial volume and the EMI) and the position of the nearest actual recorded hit in the EMI, the confidence levels C_H of the track being a hadron and C_μ of the track being a muon are calculated. The track is taken as an identified muon if it has $C_H < 10\%$ and $C_\mu > 4\%$.

Antineutrino Energy Determination: In the charged current events the antineutrino energy is the sum of the momenta in the neutrino direction of the muon, charged hadrons and neutral hadrons. For

antineutrino interactions on the average only ~ 25% of the total energy goes into hadrons ($\langle y \rangle \geq 0.25$) and only about one-third of that into neutral hadrons. In this experiment a large fraction of the neutral energy is undetected. The following is a procedure to correct the antineutrino energy for the energy missing in neutrals.

Assume that on the average the neutral hadrons in the hadron shower are symmetrically distributed around the mean charged hadron direction. Then for a sample of events, with a certain average fraction of the hadronic shower momentum undetected, on the average the same fraction of longitudinal momentum, P_L^H , and transverse momentum, P_T^H , will be undetected. Due to Fermi motion and undetected nuclear fragments we do not expect transverse momentum balance in individual events. However for a sample of events if there were no missing neutrals the mean transverse momentum of the muon $\langle P_T^H \rangle$ and hadrons $\langle P_T^H \rangle$ should balance in the antineutrino-muon plane. Therefore the mean transverse imbalance in the antineutrino-muon plane is used to correct for the missing hadronic longitudinal momentum.

We calculate the corrected antineutrino energy as follows. The uncorrected energy transfer between the leptons and hadrons ν_u from the visible energy deposited in the detector is given by

$$\nu_u = \sum P_L^H$$

where P_L^H and P_L^H are the longitudinal momentum of the muon and hadrons.

For fixed intervals of ν_u calculate $f = \langle P_T^H \rangle / \langle P_T^H \rangle$ in the antineutrino-muon plane and $\langle \nu_u \rangle$. The mean corrected energy transfer ν_c for each interval is given by

$$\langle \nu_c \rangle = \frac{\langle \nu_u \rangle}{f}$$

The mean corrected energy transfer for intervals of the mean uncorrected energy transfer is given in Figure 2. The distribution is well fitted by the correction formula $\nu_c = 1.2 (\nu_u + 1.0)$. All events are corrected for missing hadronic energy using the correction formula.

We see the correction involves a 20% scaling plus an additive 1.2 GeV which could account for unseen nuclear recoil and spallation nucleons. The antineutrino energy is then the sum of the muon energy and the corrected hadronic energy.

INDIRECT TESTS OF NEW PARTICLE PRODUCTION

A. x and y Distributions

Consider the antineutrino-nucleon interaction described by the antineutrino and muon with energies E and E_μ and a virtual boson propagator carrying the energy $\nu = E - E_\mu$ and four momentum $Q^2 = 4EE_\mu \sin^2 \frac{\theta_{\mu\nu}}{2}$. The scaling variables are defined as $x = Q^2/2m\nu$ and $y = \nu/E$. In the scaling region the cross section for "neutrino" - nucleon scattering is of the form

$$\frac{d\sigma^{\nu, \bar{\nu}}}{dx dy} = \frac{G^2 M E}{\pi} \left[F_2(x) (1-y) + 2xF_1(x) \frac{y^2}{2} + xF_3(x)y(1 - \frac{y}{2}) \right]$$

where F_1 , F_2 and F_3 are the hadronic structure functions. Assuming charge symmetry invariance and the Callan-Gross relation ($F_2(x) = 2 \times F_1(x)$) the cross section can be written:

$$\frac{d\sigma^{\nu}}{dx dy} = \frac{G^2 M E}{\pi} \left[q(x) + \bar{q}(x) (1 - y)^2 \right] \quad (1)$$

$$\frac{d\sigma^{\bar{\nu}}}{dx dy} = \frac{G^2 M E}{\pi} \left[\bar{q}(x) (1 - y)^2 + q(x) \right] \quad (2)$$

with $q(x) = \frac{1}{2} [F_2(x) + xF_3(x)]$ and $\bar{q}(x) = \frac{1}{2} [F_2(x) - xF_3(x)]$. Within the quark-parton model $q(x)$ and $\bar{q}(x)$ are interpreted as the probabilities of the quark and antiquark being involved in the interaction and carrying the momentum fraction x . The relative momentum fraction of the nucleon carried by the antiquarks is expressed in the jargon of this subject by

$$B(x) = \frac{x F_3(x)}{F_2(x)} = 1 - \frac{2 \bar{q}(x)}{q(x) + \bar{q}(x)}$$

Re-expressing equations 1 and 2 in terms of B and integrating over x gives

$$\frac{d\sigma^{\nu}}{dy} = \frac{G^2 M E}{\pi} \int F_2(x) dx \left[(1 - y + \frac{y^2}{2}) + B y (1 - \frac{y}{2}) \right] \quad (3)$$

$$\frac{d\sigma^{\bar{\nu}}}{dy} = \frac{G^2 M E}{\pi} \int F_2(x) dx \left[(1 - y + \frac{y^2}{2}) + B y (1 - \frac{y}{2}) \right] \quad (4)$$

As seen from equations 1 and 2 if the antiquark contribution to the interaction is negligible then the neutrino y -distribution will be constant and the antineutrino y -distribution will be $(1 - y)^2$. A sensitive determination of B comes from the antineutrino y -distribution in the high- y region which is dominated by the antiquark contribution. We also expect the relative antiquark contribution to affect primarily the low x region ($x < 0.2$) because of the rapidly decreasing ratio of $x F_3(x)/F_2(x)$ for small x .⁵

Let us now look at the experimental data for the y -distributions. The following data cuts were applied to the 3000 candidates described in the data analysis section to produce an unbiased antineutrino data set with well determined parameters:

1. Identify μ^+ : One positive track must be identified by the EMI as a muon, i.e., $C_H < 0.10$ and $C_\mu > 0.04$.
2. Cut neutral background (n , K^0 , etc.): Previous studies⁶ show that most of the neutron, K^0 , and other neutral background has an energy of less than 10 GeV. Therefore we require $E_c > 10$ GeV.
3. Well measured events: Require the event be greater than 65 cm from the downstream wall of the chamber to allow adequate measurement length for the tracks.
4. Good EMI Efficiency: For good EMI acceptance and to reduce hadron background we require that the muon candidate have a momentum greater than 4 GeV.
5. Good resolution of ν_c : Events with $\nu_u < 1$ GeV are cut from the sample (1) because of the large fractional correction for missing hadron energy⁷ and (2) because the small ν region is biased from the scanning loss of elastic events.

Applying these data cuts to the antineutrino candidates produced 493 charged current antineutrino events between 10 GeV and 200 GeV. The y -distribution for these events has been corrected for the EMI geometrical efficiency which was calculated using Monte-Carlo events. The EMI geometrical efficiency as a function of x and y is given in Table I.

TABLE I
EMI Geometrical Acceptance Variation with x and y
for Mean Antineutrino Energy of 20 GeV

$x \backslash y$	0.0 - 0.2	0.2 - 0.4	0.4 - 0.6	0.6 - 0.8	0.8 - 1.0
0.0 - 0.2	0.98	1.00	0.95	0.94	0.96
0.2 - 0.4	0.94	0.99	0.93	0.88	0.96
0.4 - 0.6	0.93	0.94	0.93	0.81	0.80
0.6 - 0.8	0.96	0.96	0.79	0.75	0.73
0.8 - 1.0	0.43	0.36	0.25	0.21	0.19

The y -distribution for all events between 10 GeV and 200 GeV with $0.0 < x < 1.0$ is inconsistent with a pure $(1 - y)^2$ distribution. A maximum likelihood fit gives $B = 0.79 \pm 0.06$. The y -distribution for $0.0 < x < 1.0$ and the different antineutrino energy intervals 10-30 GeV and 50-200 GeV are given on Figures 3a, 3b and 3c respectively and are compared with the theoretical y -distribution with $B = 0.8$. No apparent variation with energy is observed. The mean antineutrino energy in the 50-200 GeV distribution is about 62 GeV. Note that the fitted range of the y -distribution as shown by the data points on Figure 3 vary with antineutrino energy consistent with the $\nu_{\mu} > 1$ GeV and $P_{\mu} > 4$ GeV data cuts. The maximum likelihood fit to the y -distributions in the three energy intervals was made and the B values are given as a function of energy on Figure 4. From these data alone there is no evidence of an energy dependence of B . The data are

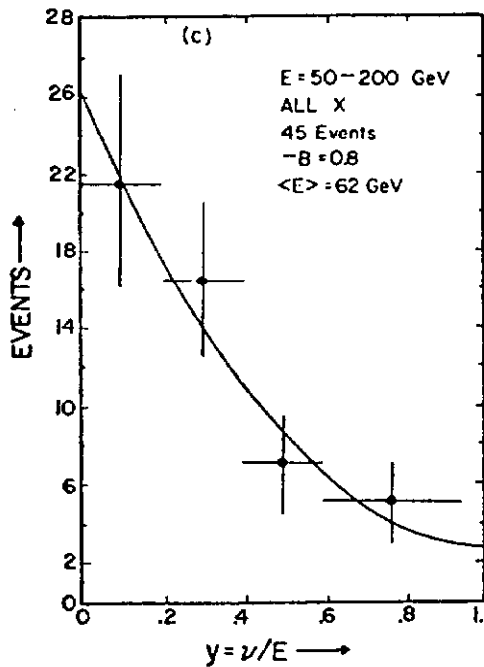
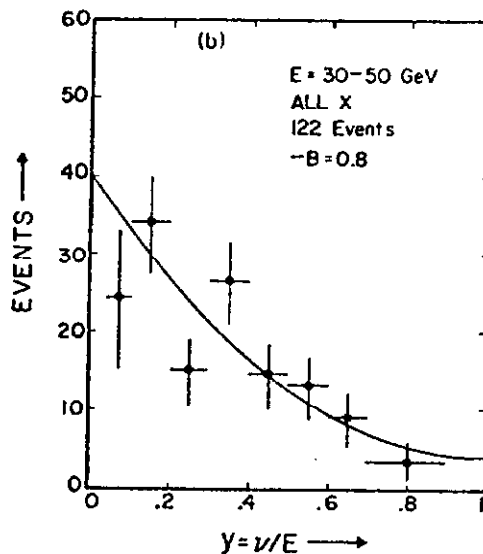
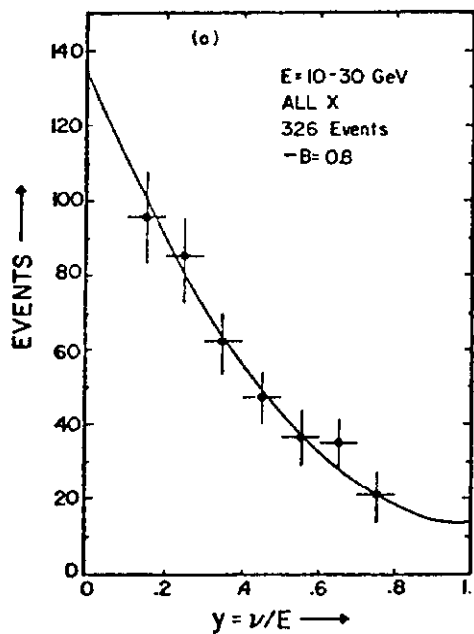


Fig. 3: Antineutrino y -distributions for events with $0 < x < 1.0$ in the antineutrino energy intervals:

- (a) $10 < E < 30$ GeV
- (b) $30 < E < 50$ GeV
- (c) $50 < E < 200$ GeV

The solid line is from Eq. 4 normalized to the data and with $B = 0.8$.

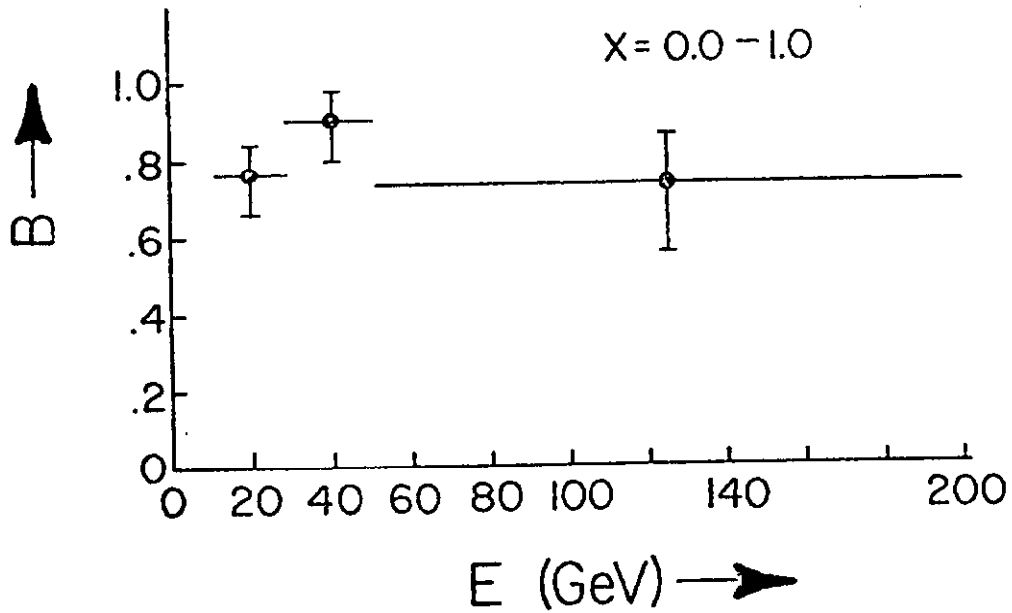


Fig. 4: B values as a function of antineutrino energy from maximum likelihood fits to data of Fig. 3a, 3b and 3c. The data are plotted in the middle of the energy intervals.

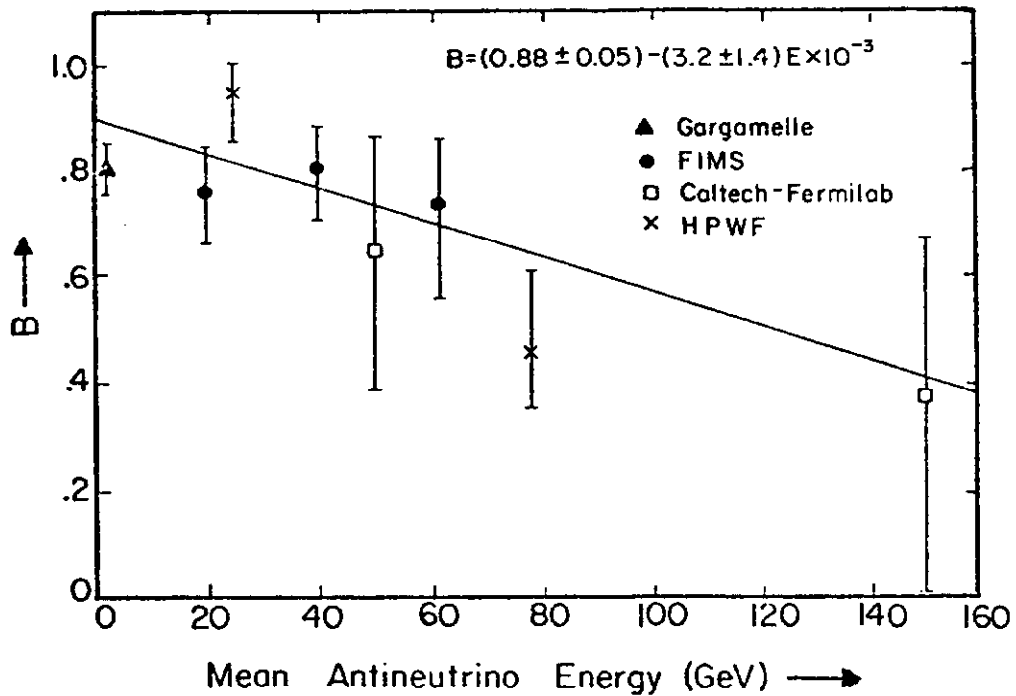


Fig. 5: B values as a function of antineutrino energy from Table II. The data are plotted at the mean of the energy interval. Solid curve is a least squares fit to the world data.

consistent with $B = 0.79 \pm 0.06$ independent of energy which gives a relative antiquark contribution to the interaction $\frac{\bar{q}}{q + \bar{q}} = 0.10 \pm 0.03$.

Let us compare the world data on B values for antineutrino interactions as a function of energy. Table II summarizes the present situation. The graphical presentation of these data is given in Figure 5. A least squares fit gives⁸

$$B = (0.88 \pm 0.05) - (3.2 \pm 1.4) E \times 10^{-3}.$$

TABLE II

B Values from Antineutrino Experiments

Experiment	Approximate Mean Energy (GeV)	Fitted B Value $B = 1 - \frac{2\bar{q}}{q + \bar{q}}$
This experiment	20	$0.76 \begin{matrix} + 0.08 \\ - 0.10 \end{matrix}$
Fermilab-ITEP-Michigan-Serpukhov (FIMS)	40	$0.90 \begin{matrix} + 0.08 \\ - 0.10 \end{matrix}$
	62	$0.73 \begin{matrix} + 0.12 \\ - 0.18 \end{matrix}$
Gargamelle (GGM) ⁹	1.5	0.80 ± 0.06
Caltech-Fermilab (CF) ¹⁰	50	$0.64 \begin{matrix} + 0.22 \\ - 0.26 \end{matrix}$
	150	$0.36 \begin{matrix} + 0.30 \\ - 0.36 \end{matrix}$
Harvard-Penn-Wisconsin-Fermilab (FPWF) ¹¹	25	0.95 ± 0.10
	78	$0.45 \begin{matrix} + 0.15 \\ - 0.10 \end{matrix}$

Consider now the x dependence of B as determined from the y-distribution. For each of the three energy intervals of Figure 3 a maximum likelihood fit to B was made to the y-distributions for the x intervals 0.0-0.1, 0.1-0.2, 0.2-0.4 and 0.4-1.0. The fitted B values are given in Figure 6. Assuming that B is not a function of antineutrino energy, the data of Figure 6 are folded together to give the x dependence of Figure 7. Also given in Figure 7 is the x dependence

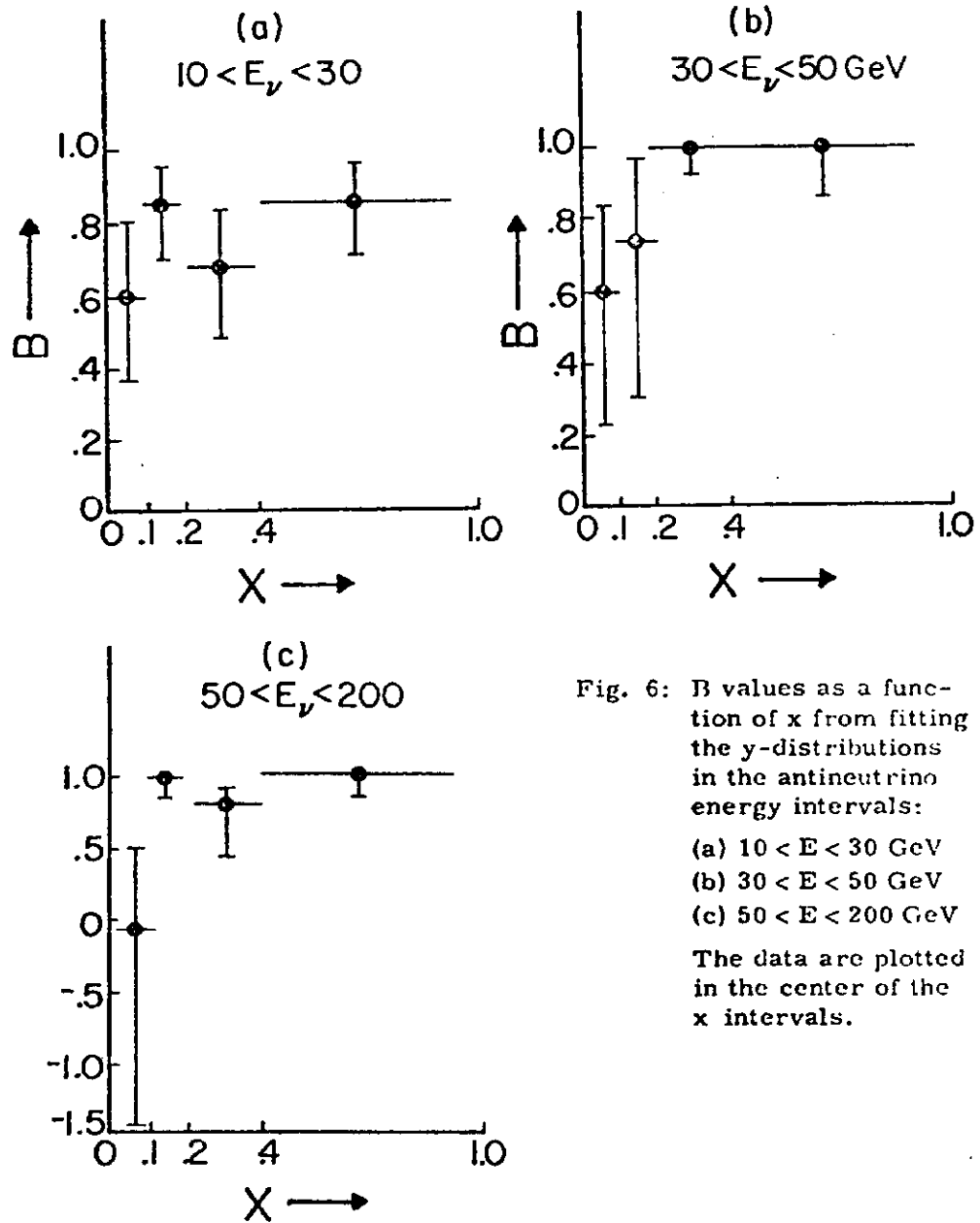


Fig. 6: B values as a function of x from fitting the y-distributions in the antineutrino energy intervals:
 (a) $10 < E < 30 \text{ GeV}$
 (b) $30 < E < 50 \text{ GeV}$
 (c) $50 < E < 200 \text{ GeV}$
 The data are plotted in the center of the x intervals.

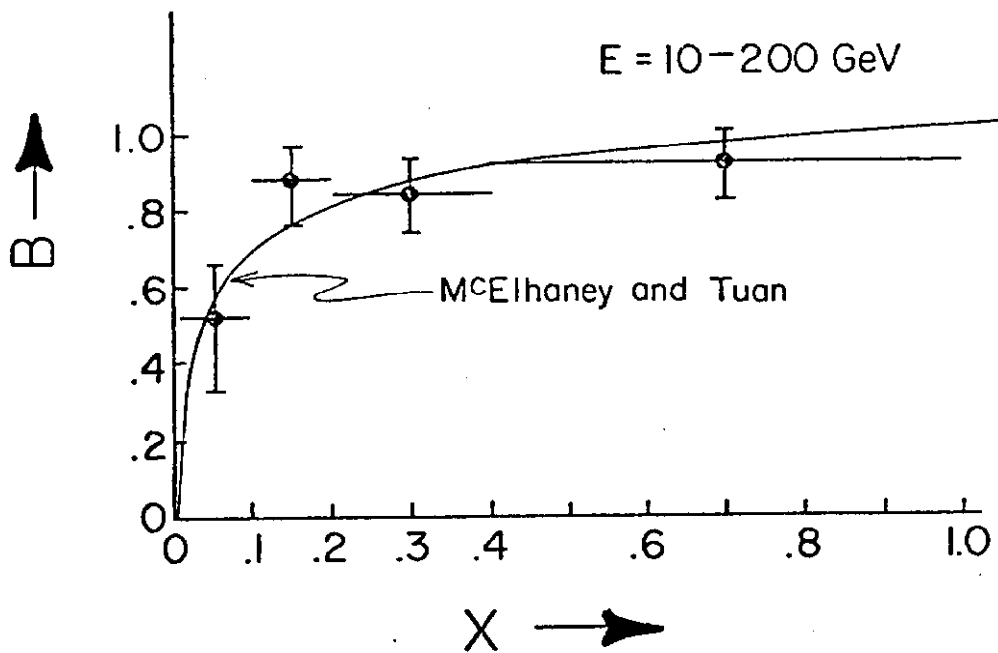


Fig. 7: Fitted B values as a function of x for antineutrino events for all energies, $10 < E < 200$ GeV.

of B as predicted by McElhancy and Tuan¹² which also fits well the Gargamelle data⁹. Even at high energies the antiquark contribution to the interaction is dominant at small x, ($x \lesssim 0.15$).

The $x = Q^2/mv$ distribution (quark momentum distribution) will be examined for three antineutrino energy intervals; 10-30 GeV, 30-50 GeV and 50-200 GeV. The x-distributions are corrected for FMI geometrical acceptance. For each energy interval only the events in the y-range unaffected by the P_μ and v_u cuts are used. For example in the $10 < E < 30$ GeV ($50 < E < 200$ GeV) range $y_{\min} = v_c^{\min}/10$ GeV = $2.4/10 = 0.3$ (0.1) and $y_{\max} = E - P_\mu^{\min}/E = 10-4/10 = 0.6$ (0.9). The x-distributions for the three energy intervals are given in Figure 8. The data are compared with F_2^{ed} (SLAC)¹³ normalized for $x > 0.2$ where the antiquark contribution in the antineutrino data is negligible. In all three x-distributions, the data show an excess of events compared to F_2^{ed} for $x < 0.2$ and good agreement for $x > 0.2$. Is this low x behavior an anomaly? Probably not!

Expressing the differential cross section for antineutrino-nucleons and electron-nucleons in terms of the weights of up quarks (u), down quarks (d), and strange quarks (s) gives

$$\frac{d\sigma^{\bar{\nu}N}}{dx} \propto u + d + 3(\bar{u} + \bar{d}) \cos^2\theta_c + 6\bar{s} \sin^2\theta_c$$

$$\frac{d\sigma^{\text{e}N}}{dx} \propto u + d + (\bar{u} + \bar{d}) + \frac{2}{5}(s + \bar{s}).$$

Assuming all the sea components have equal weight and neglecting the Cabbibo angle gives:

$$\frac{d\sigma^{\bar{\nu}N}}{dx} \propto u + d + 3(\bar{u} + \bar{d})$$

$$\frac{d\sigma^{\text{e}N}}{dx} \propto u + d + \frac{7}{5}(\bar{u} + \bar{d})$$

Therefore in the region where the antiquark contribution is negligible ($x > 0.2$) we expect agreement between the antineutrino x-distribution and the electron x-distribution. As the antiquark contribution

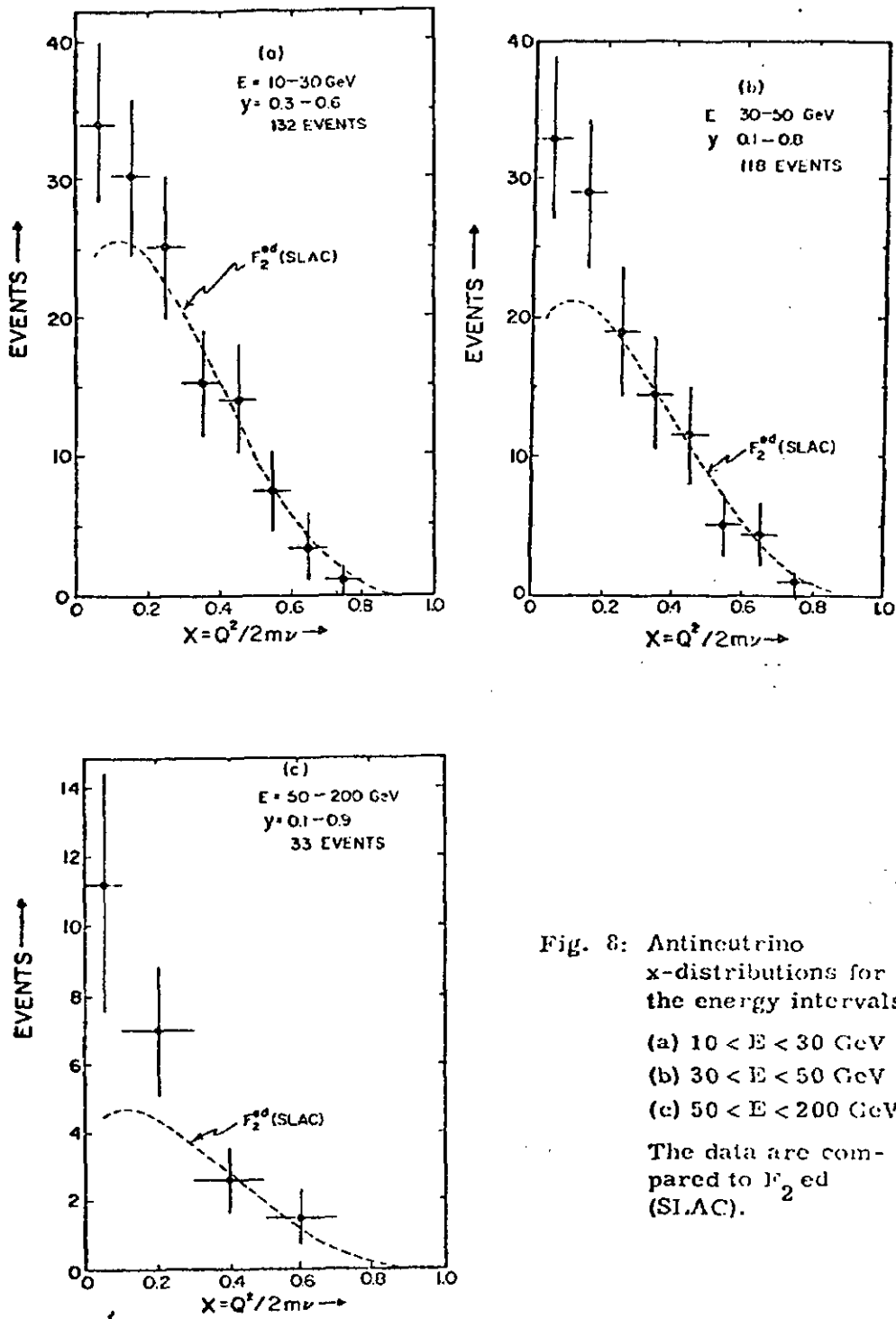


Fig. 8: Antineutrino x-distributions for the energy intervals:
(a) $10 < E < 30 \text{ GeV}$
(b) $30 < E < 50 \text{ GeV}$
(c) $50 < E < 200 \text{ GeV}$
The data are compared to F_2^{*d} (SLAC).

becomes important ($x < 0.2$) we expect the antineutrino x -distribution to lie above $F_2^{cd}(x)$. The B values determined from the antineutrino excess at low x are in agreement (within errors) with the B values determined from the y -distribution.

B. Properties of Events with Neutral Strange Particles

This is a very preliminary analysis of events with neutral strange particles produced by antineutrino interactions. Most of the events are produced from a nuclear target (Ne). No correction is at present made for nuclear absorption, etc.

All events with two-prong "associated" secondary stars were considered as events with V^0 (Λ^0 , K_s^0) candidates. All V^0 candidates were processed through Hydra geometry and through Hydra kinematics for three-constraint kinematic fits to the K^0 or Λ^0 mass hypothesis. Eighty-five events were found inside the 21 m^3 fiducial volume of the chamber which fit either K^0 or Λ . Requiring that the antineutrino energy be greater than 10 GeV and that there be an EMI identified muon in the event produced a charged current sample of 588 events¹⁴ of which 41 contain a K^0 and/or a Λ . The energy distribution of the V^0 events is given on Figure 9. The dashed line gives the shape of the energy distribution of the antineutrino charged current events in this experiment. There is no strong energy threshold above 10 GeV for a new strange particle production channel.

What is the relative rate of neutral strange particles produced in antineutrino-nucleon interactions? The observed distribution of V^0 events is given in Table III. The events with a Λ^0 or K^0 are considered observed if they have kinematic fits to $\Lambda^0 + p\pi^-$ or $K^0 + \pi^+\pi^-$. For example there were five events with an identified K^0 and an identified Λ^0 , i.e. two V^0 's. The corrections for neutral decay modes and for particles decaying outside the chamber are given in Table IV. The distribution of the corrected number of V^0 events is given in Table III.

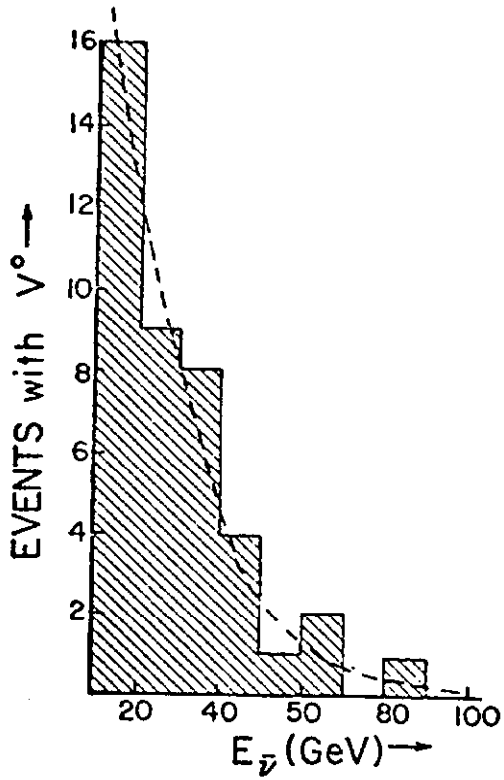


Fig. 9: Energy distribution of V^0 events.

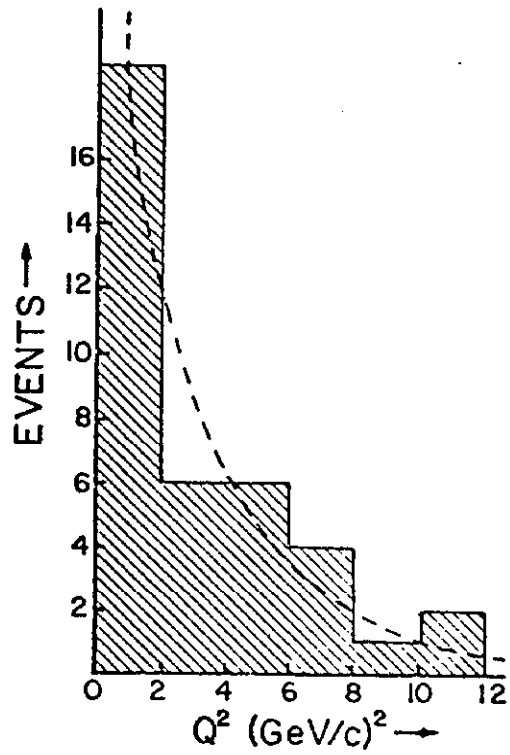


Fig. 10a: Q^2 distribution of V^0 events.

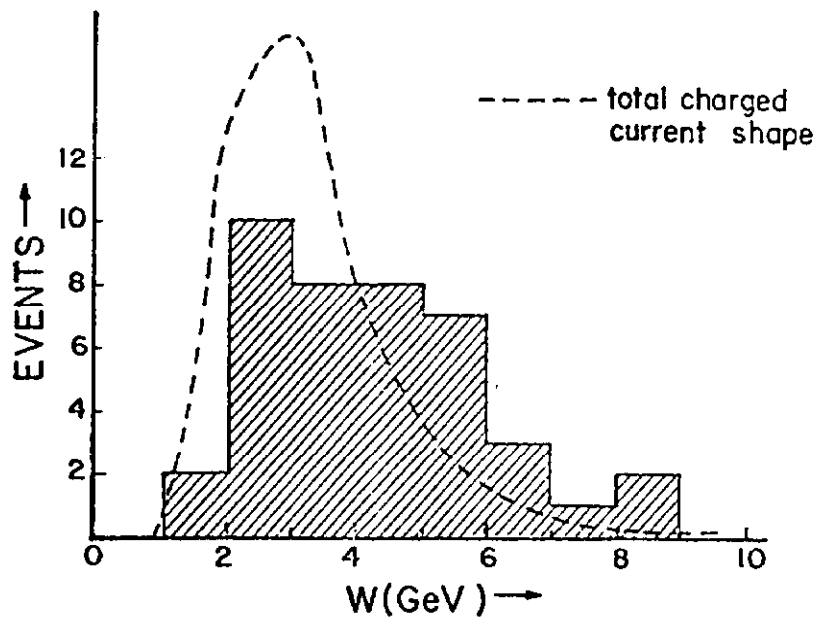


Fig. 10b: W distribution of V^0 events.

TABLE III

The Observed and Corrected Distribution of Neutral Strange Particle Events

Class	Number of Events	
	Observed	Corrected
Λ^0	21	$17 \pm 9.$
K^0	14	22 ± 17
$K^0 + \Lambda^0$	5	22 ± 10
$K^0 + K^0$	1	9 ± 9
TOTAL	41 ± 6.4	70 ± 13

TABLE IV

Probability of Observing Strange Particle Decay Mode A Coming from Source B

A \ B	Λ^0	K^0	$\Lambda^0 + K^0$	$K^0 + K^0$
	Λ^0	2/3	0	4/9
K^0	0	1/3	1/9	4/9
$K^0 + \Lambda^0$	0	0	2/9	0
$K^0 + K^0$	0	0	0	1/9

Applying additional corrections of 10% for the loss of V^0 which decay too close to the event vertex to be resolved and 10% for V^0 events lost from processing inefficiency gives the total corrected number of 85 ± 16 events containing one or more V^0 's in the charged current sample of 588 events. Therefore $(14.5 \pm 3)\%$ of the charged current antineutrino-nucleon events above 10 GeV contain one or more neutral strange particles. In a previous experiment¹⁶ it was found that $(16 \pm 3)\%$ of the charged current neutrino-proton events above 10 GeV contain one or more neutral strange particles.

The momentum transfer, Q^2 , distribution and invariant mass, W , distribution are given in Figure 10 and compared with the total charged current distributions. There is a tendency for the strange particle events to be produced at slightly higher W than the charged current events. This tendency was not statistically significant in the neutrino-proton V^0 interactions.¹⁶ The V^0 enhancement with increasing W can be better seen in Figure 11. It is clear that strange particle production does increase with increasing W and to first order the increase is independent of the particle which excites the nucleon be it a neutrino, antineutrino, photon or electron. The x and y distributions for the neutral strange particle events are given in Figure 12 and are compared with the shape of the total antineutrino charged current event sample. The shaded part of the distribution represents the V^0 events with $W > 5$ GeV. The total V^0 sample has an x and y distribution consistent with the charged current events. However, the V^0 events with $W > 5$ GeV are concentrated at higher than average y values.

DIRECT TESTS OF NEW PHENOMENA

A. Search for μ -e Events

Recently evidence has been reported^{17,18} for neutrino induced events with both a positron and a negative muon in the final state. At high energy these events are reported to occur at a level of ~1% of all neutrino interactions. There is evidence that the rate of strange particle production in these events is anomalously high. Herein we report on a search for similar events produced in the antineutrino experiment.

The antineutrino events were selected as described in the Data Analysis section. After the events were measured, all events with $\Sigma P_x > 7.5$ GeV/c were examined by physicists searching for evidence

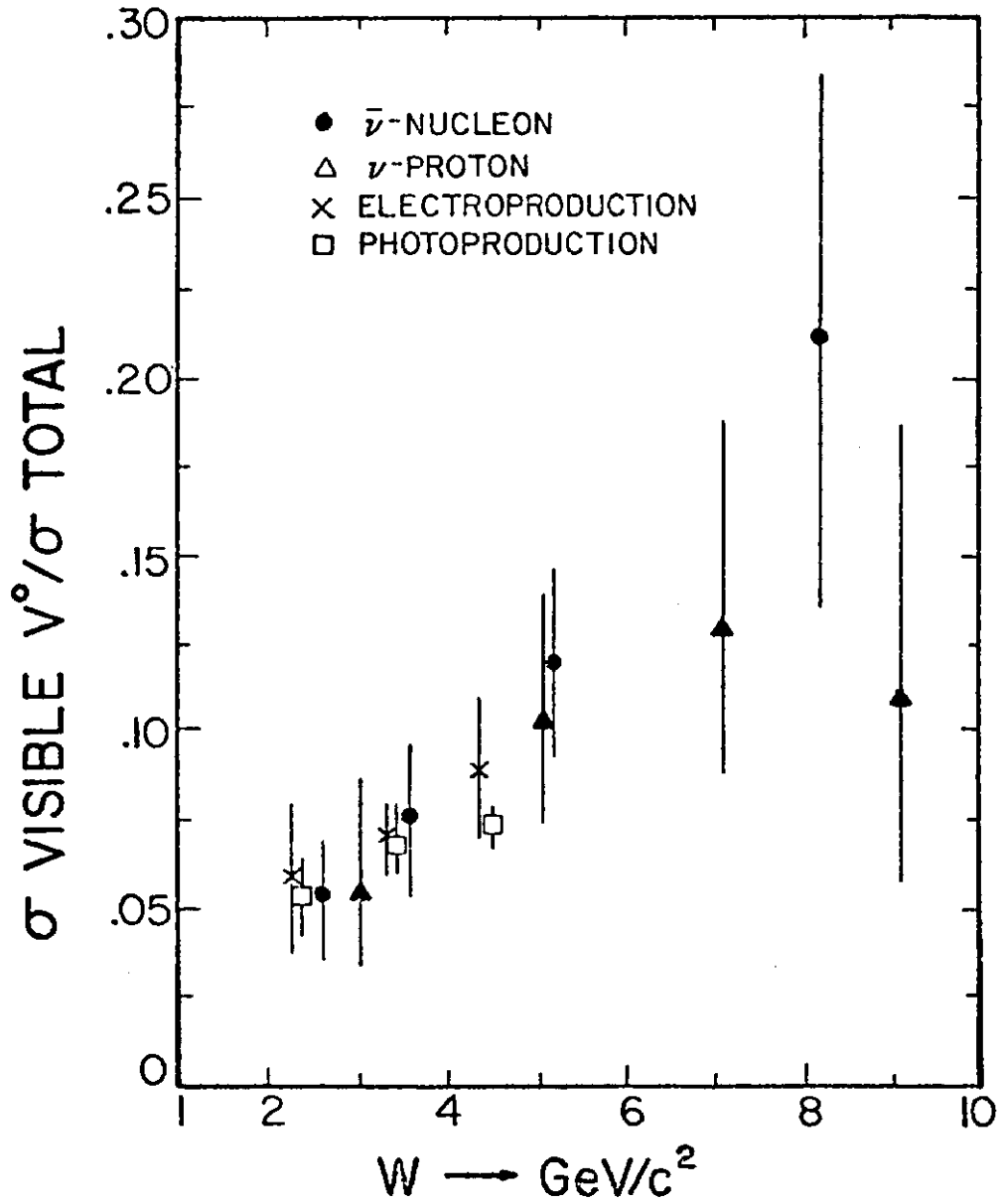


Fig. 11: The relative fraction of antineutrino charged current events with V^0 's as a function of W . Comparison is made with neutrino-proton interactions, electroproduction and photoproduction.

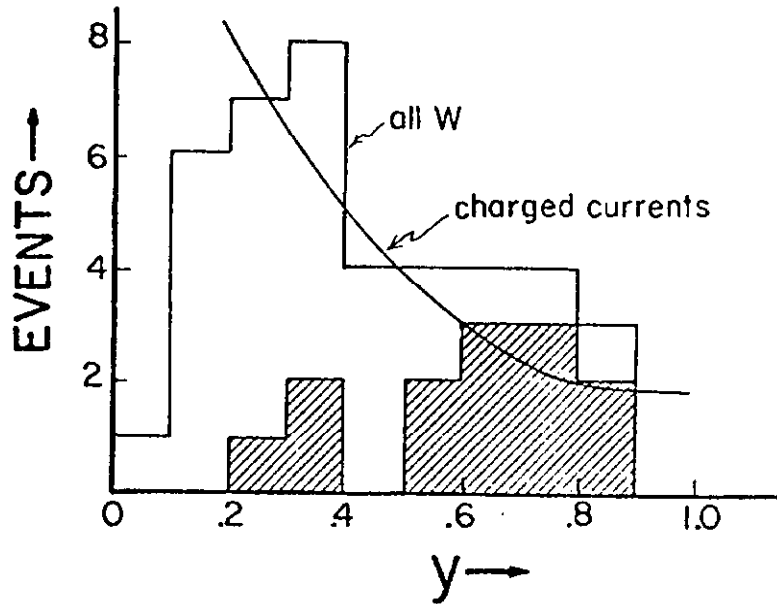
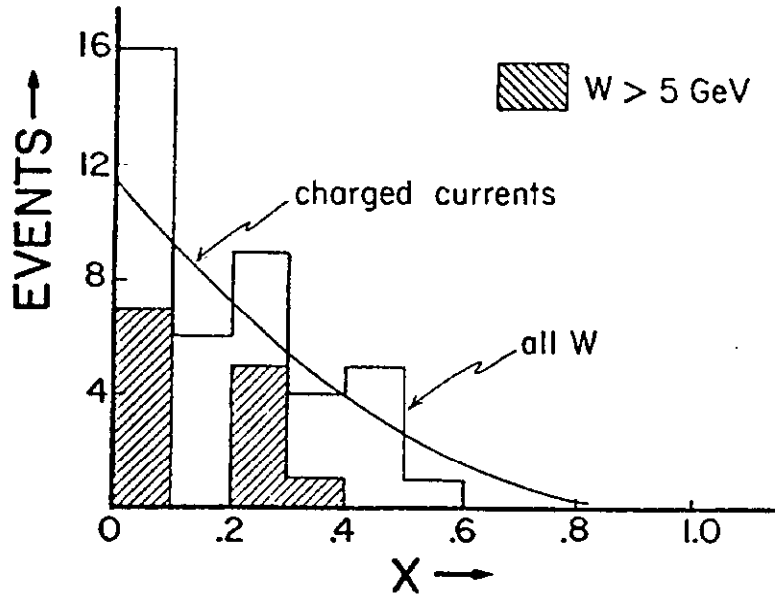


Fig. 12: x and y distributions for all V^0 events. The solid curve shows the shape of the total charged current x and y distributions. The shaded area shows V^0 events with $W > 5$ GeV.

of electrons or positrons at the primary vertex. Each track was examined carefully under high magnification (X70) over its entire length. Any track which spiralled smoothly to a point in the liquid or which had any visual indication of catastrophic energy loss - bremsstrahlung (sudden curvature changes and/or converted pairs), tridents, large δ -rays, or annihilation (in the case of positrons) - was considered an electron or positron candidate. Each electron or positron candidate was measured and fitted over its entire length to find evidence of radiative energy loss. Electron or positron candidates which showed definite evidence of energy loss inconsistent with any other mass assignment were considered as identified.

In order to measure the detection efficiency for electrons produced with the same spatial distribution as the events in the bubble chamber, physicists examined both tracks of each electron-positron pair produced within 20 cms of the primary vertex of an event. Each track was examined to see whether it would have been classified as an electron or positron candidate using the same criteria as were used for tracks from the primary vertex. Figure 13 shows the measured electron detection efficiency as a function of the electron energy E_e . This efficiency decreases with increasing E_e to an approximately constant value of 0.70 ± 0.08 for $E_e > 800$ MeV.

As the electron energy decreases the number of expected background events becomes large as discussed below. Therefore events with electrons or positrons at the interaction vertex with $E_e < 200$ MeV are not considered further. After removing electron-positron pairs 12 events have an electron or positron apparently originating at the interaction vertex. These events are listed in Table V. The energies E_e are determined from curvature measurements corrected where appropriate for detected bremsstrahlung.

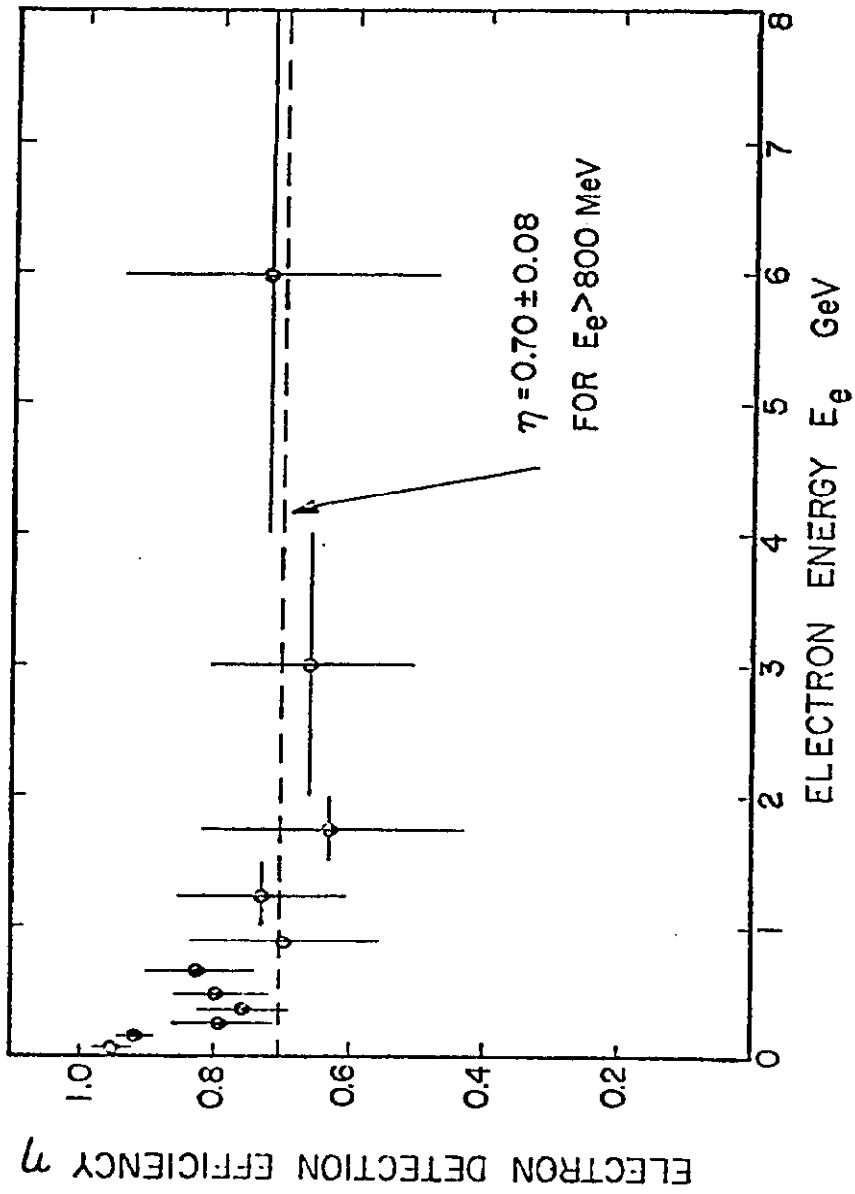


Fig. 13: The electron detection efficiency determined from a study of electron positron pairs plotted as a function of electron energy E_e .

TABLE V

List of Events with Single Electrons or Positrons
with $E_e > 200$ MeV

Event Number	ΣP_x	E_e	EMI Muon	V^0
1	26 GeV/c	1.4 ± 0.1 GeV e^+	None	None
2	8 GeV/c	2.0 ± 0.1 GeV e^+	None*	None
3	21 GeV/c	12 ± 2 GeV e^+	None	None
4	33 GeV/c	32 ± 7 GeV e^+	None*	None
5	54 GeV/c	35 ± 5 GeV e^+	8.7 GeV μ^+	None
6	56 GeV/c	56 ± 13 GeV e^+	None*	None
7	68 GeV/c	67 ± 10 GeV e^+	None*	None
8	32 GeV/c	1.2 ± 0.01 GeV e^-	17.3 GeV μ^+	None
9	10 GeV/c	6.3 ± 0.4 GeV e^-	None	None
10	42 GeV/c	31 ± 8 GeV e^-	None	None
11	55 GeV/c	37 ± 12 GeV e^-	None	4 GeV/c K_s^0
12	153 GeV/c	130 ± 40 GeV e^-	None*	None

* All secondaries identified as hadrons in the bubble chamber.

Five events have all tracks other than the electron or positron identified as hadrons in the bubble chamber. Only events 5 and 8 have a muon identified by the EMI and are considered as μe candidates. Event 11 has a 4 GeV/c K_s^0 ; no other event shows any evidence for a strange particle.

In order to assess the significance of the two μe candidates consider the following backgrounds:

1. Electron neutrinos and antineutrinos are expected to be present in the beam at about the 1% level. Events 3 through 7 and 9 through 12 in Table V have leading electrons or positrons and are very likely to be ν_e or $\bar{\nu}_e$ induced events. A ν_e or $\bar{\nu}_e$ event can simulate a μe event when a hadron is misidentified as a muon by the EMI. The

probability that a hadron is misidentified as a muon by the EMI is estimated to be ~3%. With the assumption that all the events in Table V are ν_e or $\bar{\nu}_e$ induced, this background is estimated to be ~0.03 μ^+e^+ and ~0.15 μ^+e^- events. The importance of suppressing the ν_e background is clearly evident.

2. The film quality is such that a close in Compton electron vertex (within about 2 cm of the interaction vertex) may not be resolved. This background has been estimated from the measured gamma spectrum. Figure 14 shows the expected number of charged current events with close in Compton electrons with $E_e > E_{\min}$.

3. Events with asymmetric gamma conversion within 2 cm of the primary vertex or asymmetric Dalitz pairs having an undetected electron or positron, apparently have a single positron or electron at the interaction vertex. With the assumption that electrons or positrons with $E_e < 5$ MeV are always undetected the expected number of such events has been estimated from the observed spectrum of Dalitz pairs and close in pairs and is shown in Figure 14. As E_e decreases below 200 MeV the background from both sources 2) and 3) increases rapidly.

4. Small angle K_{e3} decays are estimated from the observed number of K_S^0 decays and decay kinematics to contribute 0.02 e^- and 0.04 e^+ background events.

Event 5 is the only μ^+e^+ candidate. In addition to the μ^+ and the e^+ in this event there are two negative hadrons. Interpreted as a $\bar{\nu}_\mu$ charged current event the estimated antineutrino energy $E_{\bar{\nu}}$ is 64 GeV, and the estimates for the scaling variables are $x = 0.001$ and $y = 0.86$. However the presence of a high energy leading e^+ suggests that this event may be a $\bar{\nu}_e$ event with a positive hadron misidentified as a muon even though the expected number of such events is only ~0.03.

Event 8 is the only μ^+e^- candidate. Events of the type μ^+e^- are of the particular interest because the lepton configuration is

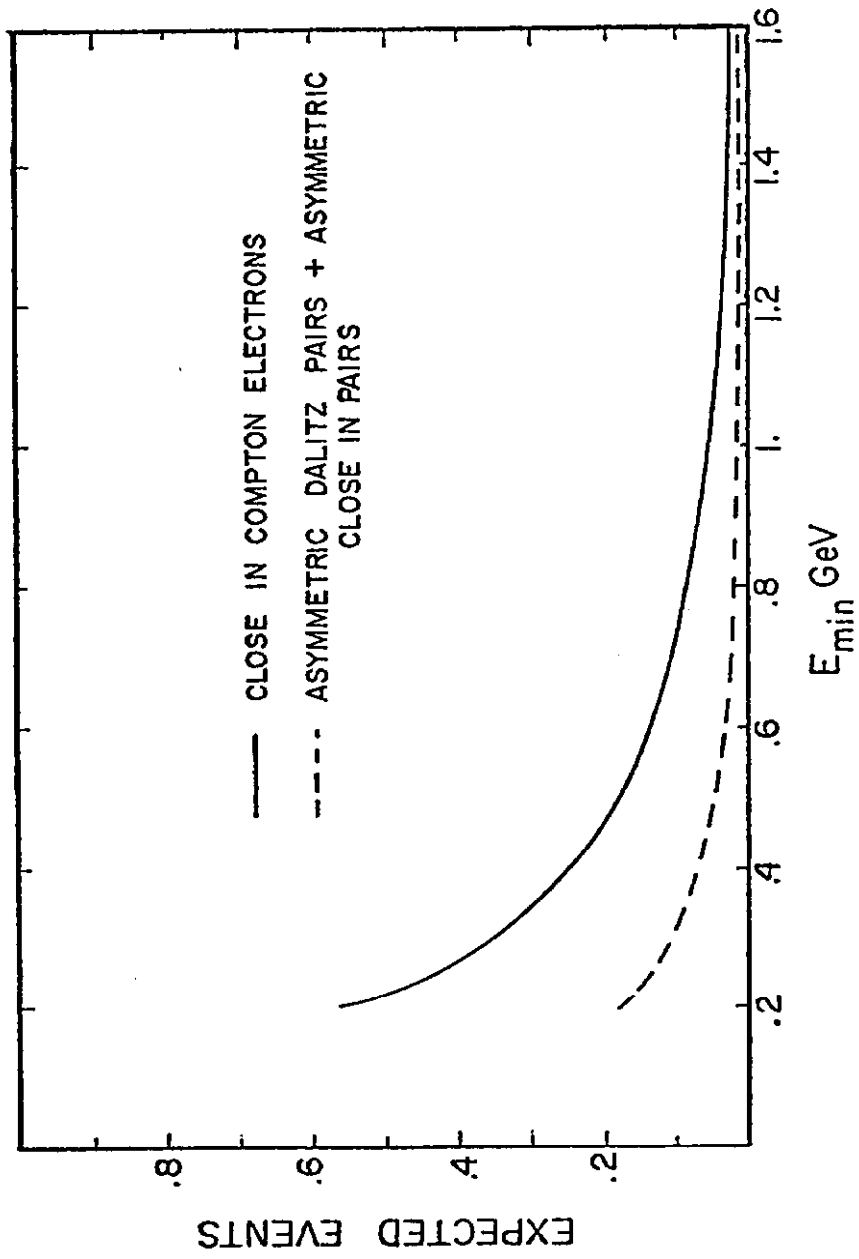


Fig. 14: The expected number of background events with $E_e > E_{min}$ due to close in Compton electrons and due to asymmetric Dalitz pairs and close in pairs.

charge conjugate to the configuration $\mu^- e^+$ observed in neutrino interactions as reported in References 16 and 17. In addition to the μ^+ and e^- there are 4 positive hadrons and 2 negative hadrons in this event. Interpreted as a $\bar{\nu}_\mu$ event the estimates for the antineutrino energy and the scaling variables are given by $E_{\bar{\nu}} = 36$ GeV, $x = 0.066$ and $y = 0.51$. The combined background from all sources 1-4 considered above for $E_e > 1.2$ GeV is 0.2 ± 0.2 events. In fact for this particular event there is a small track of unknown sign at the interaction vertex which could be a positron with energy ~ 2 MeV which would indicate that the electron is part of a very asymmetric Dalitz pair. See Figure 15. The electron track overlaps 4 other tracks at the interaction vertex and it cannot be excluded that it is due to a Compton electron. The event is not considered compelling evidence for $\bar{\nu}_\mu$ induced $\mu^+ e^-$ events.

Table VI shows the upper limit at 90% confidence for the yields of $\mu^+ e^-$ and $\mu^+ e^+$ events relative to all antineutrino charged current

TABLE VI
Upper Limits for Antineutrino Induced μe Events as a Function of Energy (90% Confidence Level)

$E_{\bar{\nu}}$	Charged Current Events	$\sigma(\mu^+ e^-)/\sigma(\mu^+ X)$	$\sigma(\mu^+ e^+)/\sigma(\mu^+ X)$	$\sigma(\mu e \nu^0)/\sigma(\mu^+ X)$
>10 GeV	1120	0.5%	0.5%	0.3%
>20 GeV	630	0.9%	0.9%	0.5%
>30 GeV	330	1.7%	1.7%	1.0%
>40 GeV	160	2.1%	3.6%	2.1%

events based on a single candidate in each case. Note that our maximum data sample has been used in this analysis. The upper limit on the relative yield of μe events with associated neutral strange particles detected via charged decay modes (ν^0) is also given based on zero



Fig. 15: High magnification view of the vertex of the $\mu^+ e^-$ candidate. The radius of curvature of the curling lepton track at the vertex is about $2 \text{ MeV}/c$.

candidates. The number of charged current events has been corrected for missing single track events.¹⁹ No correction has been applied for EMI acceptance; the assumption is made that the EMI acceptance for μe events is the same as for all other charged current antineutrino events. The upper limits have been corrected for the electron detection efficiency $\eta = 0.70$. The upper limits are applicable for electrons with energies $E_e > 200$ MeV and for muons with energy above 4 GeV.

B. Search for μ - μ Events

We will present very preliminary results on the direct dimuon production by antineutrinos interacting in hydrogen-neon. The search naturally divides itself into two studies. The first study is for the sample of dimuons where one muon is fast ($P_\mu > 4$ GeV/c) and therefore identified by the EMI and the other muon is slow and decays and is identified in the bubble chamber (fast-stopping dimuons). The second study is for the sample where both muons are fast and are identified by the EMI (fast-fast dimuons).

Fast-Stopping Dimuons: The 1157 events with $\sum P_x > 7.5$ GeV studied in the μe search are further studied here. In several independent physicist scans all events were searched for continuous tracks which terminated in an identified electron as described in the previous section. These events contained direct electrons from the primary vertex, π - μ -e decays and μ -e decays. The direct electron candidates were used in the μ -e dilepton analysis.

Here we consider the events with π - μ -e and μ -e tracks which are trapped in the bubble chamber. The bubble chamber is basically a sphere of 1.8m radius with a magnetic field of 30 Kg. In principle a 1.5 GeV/c track can be trapped within the chamber and decay. In practice however the muon trapping efficiency drops to 10% for antineutrino events for muons of 600 MeV/c (muon range of 740 cm).

Therefore in this study we restrict the slow muon to have a momentum of less than 600 MeV/c.

There were several events with very slow stopping positive tracks. In every case, these were ambiguously identified as stopping π^+ from observation of the unmistakable $\pi^+-\mu^+-e^+$ chain. We measured and fit these tracks in order to gain some appreciation of the power of our Geometry program in separating slow π^+ from slow μ^+ orbits. It was found that for stopping tracks shorter than about 15 cm, there is inadequate difference between the quality of the fits for the μ mass and the π mass assumptions to allow convincing separation. In the fast-stopping dimuon study we therefore exclude all μ candidates with $P_\mu < 0.1$ GeV/c (corresponding to a μ with residual range of 22 cm). However in the present data sample there were no muon candidate in this momentum region.

The events were scanned at almost life-size. In the 23% atomic Neon-Hydrogen mix the range of the μ from a π decay at rest is ~ 3 mm on the scanning table. Because of foreshortening due to dip and possible μ alignment with the incident direction of the decaying pion it is frequently difficult to separate the $\pi-\mu-e$ decay chain from the $\mu-e$ decay at rest. Since it is difficult to visually detect angle changes less than 5° on a slow track, it is impossible to separate $\pi-\mu$ decays in flight with a trapped μ subsequently decaying at rest from $\mu-e$ decays. For these reasons the nature of the track ending in an electron was in most cases not determined at the scanning stage.

We measured every candidate track that did not have an unambiguous $\pi-\mu-e$ or an obvious kink from the production point down to the electron vertex with many points per view. The tracks were then fit starting at the production vertex in increasing arc length, looking for deviation in angle and momentum of the downstream orbit from the prediction of the fit to the upstream orbit larger than that predictable from multiple

scattering. This process largely eliminates π - μ decays in flight. In the remaining events, the transition point between the parent track and the electron track was discernable. Using the range-momentum relation for pions and muons allowed the separation of the remaining sample into probable stopping pions with invisible daughter muons and probable stopping muons. Three probable stopping muon events were found.

The properties of the three stopping muon events are given in Table VII. Events 2 and 3 are interpreted as antineutrino charged current high- γ events with γ values of 0.990 and 0.985. Observing two high- γ events is consistent with $B = 0.8$. Event 1 is an apparent $\mu^+\mu^+$ event. Observing one such event is consistent with the estimated

TABLE VII

Properties of Antineutrino-Nucleon Events with Identified Stopping Muons

Event No.	ΣP_X	Stopping Muon Momentum	Fast EMI Muon Momentum
1	11.4 GeV	170 MeV/c μ^+	6 GeV/c μ^+
2	17.8 GeV	174 MeV/c μ^+	None
3	8.2 GeV	126 MeV/c μ^+	None

background from early and small angle π - μ decay in flight. No $\mu^+\mu^-$ events were found with one fast muon ($P_\mu > 4$ GeV/c) and one or more slow muons ($P_\mu < 0.6$ GeV/c). For antineutrino energies greater than 10 GeV a 90% confidence level upper limit on the production rate of $\mu^+\mu^-$ events within the above momentum ranges is about 3% of all charged current events. This limit has been corrected for the geometrical trapping efficiency for the slow stopping muon and for the μ^- capture probability. The $\mu^+\mu^-$ background is estimated to be about 0.3 events with the above cuts.

Fast-Fast Dimuons: We report here preliminary results on a search for events with two or more tracks identified as muons by the EMI. The data set used here is approximately the same as used in the μ -e search. The previously described EMI muon selection procedure ($C_{II} < 10\%$, $C_{\mu} > 4\%$ and $P_{\mu} > 4$ GeV) was applied to each leaving track of the event which did not interact in the chamber. An acceptable multiple muon candidate satisfied the following conditions: the muon candidates did not have the same hit in the EMI, the time coincidence of "muon hits" in the EMI was within 111 nsec, each muon candidate had a momentum greater than 4 GeV/c and the total antineutrino energy was greater than 10 GeV. With these conditions the total efficiency for detecting the leading muon is ~75%. The total efficiency for detecting the non-leading muon is ~70%. Eleven dimuon candidates were found which satisfied the above conditions: 1(++), 5(+), 5(-) and 0(--), where the signs refer to the charge of the leading and non-leading muon candidates.

The dominant background in this procedure to select dimuon events is the normal charged current event accompanied by a pion punching-through to the EMI and being misidentified as a muon. The momentum spectrum of the non-leading muon candidates was calculated by applying an estimate²⁰ of the punch-through probability to the observed spectrum of π^+ and π^- mesons in the charged current events which exit the chamber without interacting. The observed and calculated integral spectra for the non-leading muon are given in Table VIII.

TABLE VIII

Number of Observed Dimuon Candidates and Calculated Background as a Function of the Momentum P' of the Non-leading "muon"

P' (GeV/c)	N(++)		N(+--)		N(--+)		N(---)	
	obs.	calc.	obs.	calc.	obs.	calc.	obs.	calc.
> 2	3	3.5	9	5	7	3.5	0	1.1
> 4	1	2	5	3	5	3	0	0.8
> 6	0	1	3	1.5	5	2	0	0.5
> 10	0	0.3	1	0.7	3	1	0	0.2
> 20	0	0.07	0	0.25	0	0.2	0	0.1

For events with $P' > 4$ GeV/c, 11 dimuon candidates were observed with a calculated background of 8.8 events. The observed number of dimuon candidates is not statistically significant above the estimated background. Only one dimuon candidate with $P' > 4$ GeV/c ($P_{\mu^+} = 11$ GeV/c, $P_{\mu^-} = 18$ GeV/c, $E_{\bar{\nu}} = 180$ GeV) has an associated neutral strange particle, a K^0 .

Assuming all the dimuon candidates in Table VIII with $P' > 4$ GeV/c are real dimuon events and folding in the total muon identification efficiencies, the 90% confidence level upper limits for the relative rates of dimuon production with and without a V^0 in antineutrino reactions is given in Table IX. The dimuon rates are relative to the charged current sample which has been corrected for missing one-prong events. The upper limits are given in Table IX for dimuon production above antineutrino energies of 10-40 GeV.

It should be noted that assuming that the momentum spectrum of the non-leading muon in dimuon events is similar to the momentum spectrum of hadrons produced in single muon events, the requirement that the non-leading muon have $P_{\mu} > 4$ GeV will suppress the apparent dimuon rate at lower antineutrino energies (~20-30 GeV).

It is clear that this type of analysis can be improved by using higher density neon-hydrogen chamber fittings and by an improved FMI.

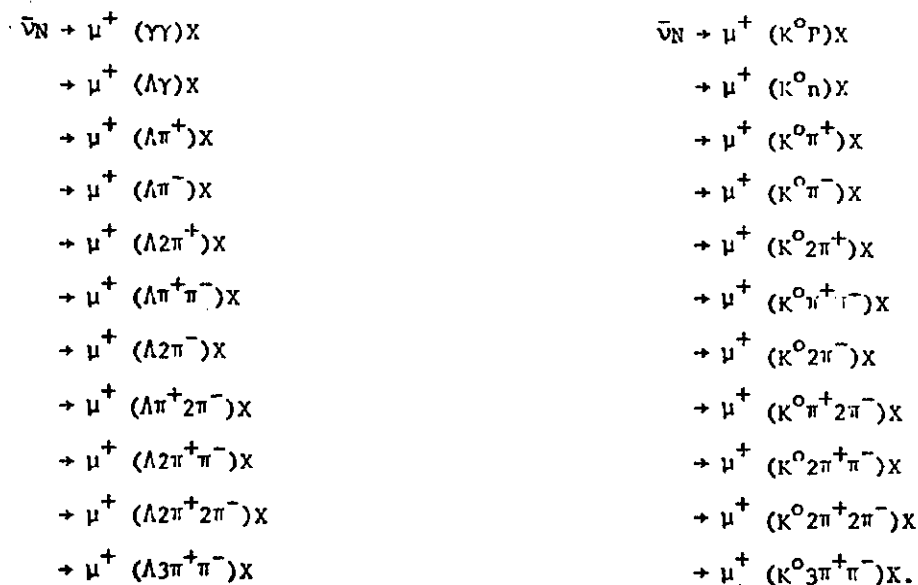
TABLE IX
90% Confidence Level Upper Limits for Antineutrino Induced Dimuon Events as a Function of Energy

$E_{\bar{\nu}}$ (GeV)	$\frac{\sigma(\mu^+\mu^-X)}{\sigma(\mu^+X)}$	$\frac{\sigma(\mu^+\mu^+X)}{\sigma(\mu^+X)}$	$\frac{\sigma(\mu^+\mu^+\nu^0)}{\sigma(\mu^+X)}$
10	1.4%	0.6%	0.35%
20	2.4	1.1	0.6
30	4.2	2.0	1.2
40	5.8	4.3	2.4

C. Study of the Strange Particle Invariant Mass Spectra

A preliminary analysis is reported on semi-inclusive invariant mass spectra of 3-7 prong charged current events above 10 GeV with one or more observed neutral strange particles. This sample consists of about 500 charged current events including 17 Λ , 12 K^0 and 2 $K^0\Lambda$ events.

Semi-inclusive invariant mass distribution, were studied for the combinations in brackets for the following reactions:



For this analysis all unidentified charged tracks were taken as pions.

The $(\Upsilon\Upsilon)$ mass distribution for all charged current events with two gamma rays is given in Fig. 16a. The π^0 peak has a width of ± 15 MeV centered at 130 MeV. The $(\Lambda\Upsilon)$ mass distribution is given in Fig. 16b. There is some indication for the production of Σ^0 (1190). A search was made of all the other invariant mass distributions for resonances with a width of ≤ 50 MeV. From a preliminary analysis, no narrow peaks were found which contained 4 or more events above background.

There is evidence from SPEAR for the existence of a charmed meson D^0 (\bar{D}^0) with a mass ~ 1.87 GeV. In antineutrino interactions we might therefore expect to produce the \bar{D}^0 which could decay $\bar{D}^0 \rightarrow \bar{K}^0 \pi^+ \pi^-$. Figure 16c shows the $(K^0 \pi^+ \pi^-)$ mass distribution. There is no evidence for the production of \bar{D}^0 by antineutrinos. The upper limit on the cross section, relative to all charged current events, times branching ratio for the mode $\bar{D}^0 \rightarrow K^0 \pi^+ \pi^-$ is about 1.5%.

CONCLUSIONS FROM ANTINEUTRINO-NUCLEON INTERACTIONS

1. y distribution study - The relative antiquark content of the nucleon is energy independent; $\frac{\bar{Q}}{Q+\bar{Q}} = 0.10 \pm 0.03$.
2. x distribution study - The x distribution is consistent with F_2^{ed} (SLAC) for $x \geq 0.2$ and is energy independent.
3. Properties of V^0 events - The relative fraction of charged current events above 10 GeV with one or more V^0 is $14.5 \pm 3\%$, increases with increasing W and is consistent with νp interactions.
4. μ -e search - The upper limit on the production of μ -e events by antineutrinos is $\frac{\sigma(\mu^+ e^- X)}{\sigma(\mu^+ X)} < 0.5\%$ for $E_\nu > 10$ GeV.

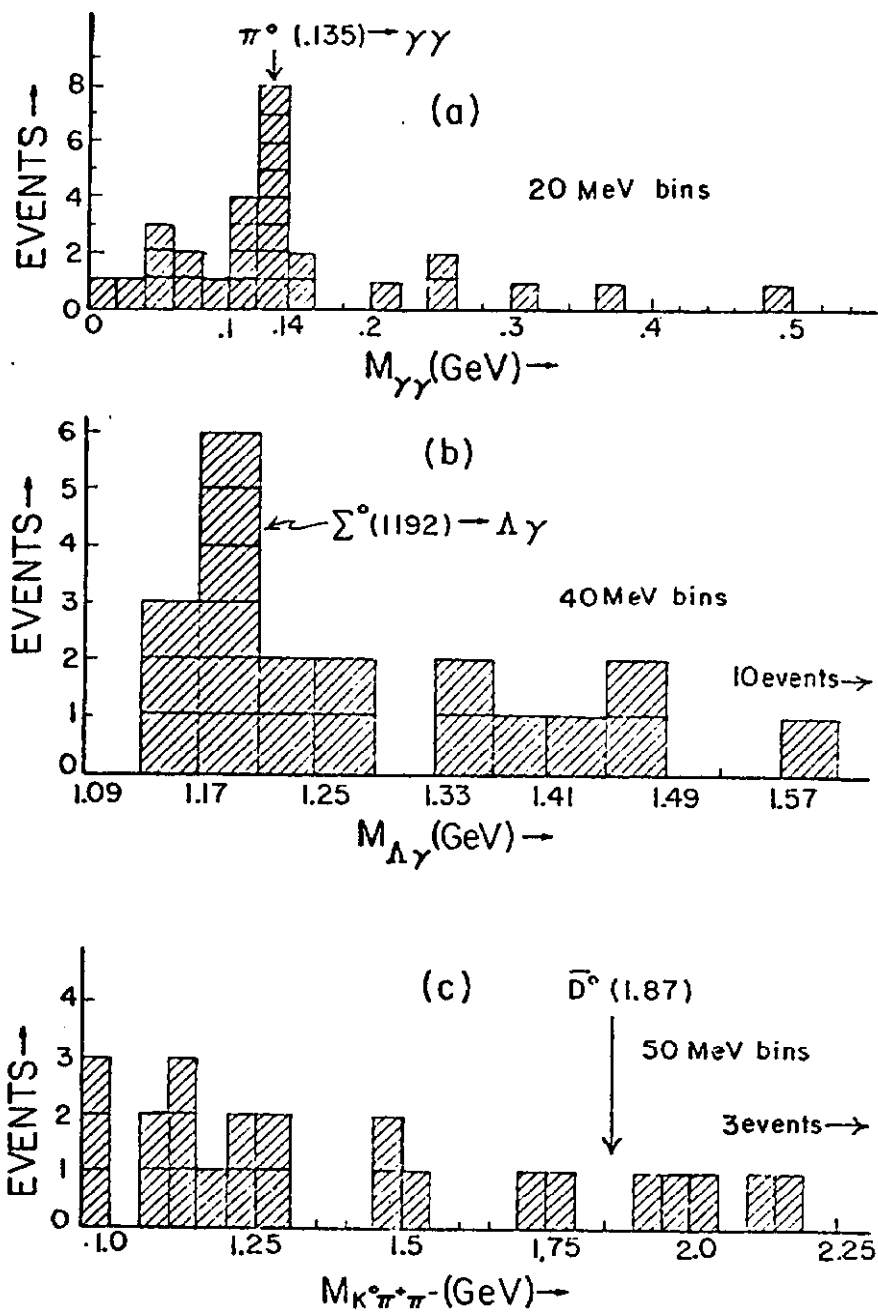


Fig. 16: Invariant mass distributions for (a) $\gamma\gamma$ combinations from all charged current events with 2 γ -rays converted. (b) $\Lambda\gamma$ distribution for all Λ events. (c) $K^0\pi^+\pi^-$ distribution for all K^0 events.

6. $\mu\text{-}\mu$ search - For antineutrino interactions greater than 10 GeV, the $\mu\text{-}\mu$ upper limit is

$$\frac{\sigma(\mu^+\mu^-X)}{\sigma(\mu^+X)} = \begin{cases} < 3\% & P_{\mu^+} > 4 \text{ GeV} & P_{\mu^-} < 0.6 \text{ GeV} \\ < 1.4\% & P_{\mu^+} > 4 \text{ GeV} & P_{\mu^-} > 4 \text{ GeV} \end{cases}$$

7. V^0 invariant mass spectra study - No evidence was found for new narrow resonances. The upper limit (cross section x branching ratio) on the relative yield of \bar{D}^0 in antineutrino interactions is 1.5%.

WHAT IS IN THE FUTURE

The present experiment based on approximately 1,000 charged current antineutrino interactions lacks the statistical sensitivity to make strong conclusions on 1) the high-y anomaly, 2) the $\mu\text{-}e$ production, 3) the $\mu\text{-}\mu$ production and 4) peaks in the strange particle invariant mass plots. During the first quarter of 1977 this experiment expects with additional running at Fermilab to increase its statistics by almost an order of magnitude. With the improved statistics and improved identification power of a heavier neon-hydrogen mixture it is anticipated that it will be possible to obtain definitive answers to some of the most important outstanding questions in present day experimental antineutrino physics.

FOOTNOTES AND REFERENCES

1. R. J. Cence, et al., University of Hawaii Report UH 511 217 76; Lawrence Berkeley Laboratory Report LBL-4816 (to be published in Nuclear Instruments and Methods).
2. In this experiment a muon is considered to be identified by the FMI if the muon confidence level for the match is greater than 4% and if the hadron confidence level is less than 10%.
3. Film copied at Eastman Kodak Co., Oakbrook, Illinois.
4. Hydra Geometry, Hydra Application Library, CERN.
5. H. Dedén, et al., Nucl. Phys. B85, 269 (1975).
6. J. W. Chapman, et al., Phys. Rev. D. 14, 5 (1976).
7. A large fractional error in v_c for small v values has a negligible effect on the $y = v/E$ distribution but a large effect on the $x = Q^2/2mV$ distribution.
8. The difference between this fit and the fit reported earlier at the 1976 International Conference on Neutrino Physics, Aachen by F. Nezzrick is the use here of the older Gargamelle determination of B determined from the y distribution study.
9. D. H. Perkins, Proceedings of the 1975 International Symposium on Lepton and Photon Interactions at High Energies, Stanford.
10. Results reported at the 1976 International Conference on Neutrino Physics, Aachen. The result was presented in terms of α where $B = 1-2\alpha$.
11. Results reported at the 1976 International Conference on Neutrino Physics, Aachen.
12. R. McElhaney and S. F. Tuan, Phys. Rev. D8, 2267 (1973).
13. A. Bodek, thesis, MIT, 1973 (unpublished).
14. Slightly different data sets have been used in the different sections of this paper. They are all unbiased sets with slightly more statistics in some studies. In each case the data set will be explicitly stated.
15. The total corrected number of V^0 events is independent of the number of observed ΛK events, i.e., $3/2 (\Lambda \text{ events observed}) + 3 (K \text{ events observed}) - 3 (KK \text{ events observed})$.
16. J. P. Berge, et al., Phys. Rev. Lett. 36, 127 (1976).
17. H. Deden et al., Phys. Lett. 56B, 361 (1975).
18. J. Von Krogh, et al., Phys. Rev. Lett. 36, 710 (1976).
19. The missing single track events are expected to be largely confined to the region of small y . The number of missing events is estimated assuming a y -distribution of the form $dN/dy = (1 + y$

+ $y^2/2$) - $B y(1 - y/2)$ with $B = 0.8$ and extrapolating to $y = 0$.
The correction is 14% for $\frac{E}{\bar{\nu}} > 10$ GeV and less at higher energies.

20. We appreciate V. Z. Peterson making available to us the results of Monte Carlo punch-through calculations performed by A. Grant at Cern.